UDC 004.021

Approaches to prediction of speckle removal efficiency for DCT-based filter

V. V. Lukin[1], O. S. Rubel [1]*, O. V. Naumenko [1], B. Vozel [2], K.Chehdi [2]
[1]National Aerospace University, Kharkov, Ukraine, [2]University of Rennes 1, Lannion, France

Several approaches to prediction of despeckling efficiency for DCT-based filter are presented and compared. The approaches allow predicting standard quantitative criteria as improvement of PSNR (IPSNR) as well as criteria of visual quality for filtered images. We propose and analyze rather accurate automatic procedures of prediction that exploit moments of a statistical parameter calculated in 8x8 pixel blocks of a given noisy image under condition that speckle parameters (or number of looks) are a priori known or pre-estimated with a proper accuracy. It is also shown that the prediction approaches are applicable to images with different intensity of speckle. Prediction based on neural network specially trained for multiplicative noise is demonstrated to be the most accurate.

Keywords: speckle, remote sensing, DCT-based filter, efficiency prediction

Introduction

Remote sensing (RS) from airborne and spaceborne carriers has found numerous applications [24]. Radar RS is applied alongside with other types of imaging systems and it provides certain benefits compared to other RS systems as ability to work during day and night and possibility to operate in bad weather conditions [15]. However, acquired radar images formed by modern synthetic aperture radars (SARs) suffer from a noise-like phenomenon called speckle that appears due to coherent imaging mode and is the most intensive for single-look SAR images [15, 26]. There are several ways to cope with speckle [15, 26]. One way is to form multi-look images that, unfortunately, leads to worse spatial resolution of registered images. Besides, for a limited number of looks (e.g., two or three) speckle can be still intensive and annoying. Another way is to perform despeckling (filtering, denoising) where numerous methods exist (see [8, 9, 26] and references therein). However, such despeckling, alongside with efficient noise removal in image homogeneous regions, might smear edges/details and destroy texture features which is undesirable. These undesirable effects appear themselves for complex structure images containing a lot of fine details and textures. Then sometimes it becomes undesirable to carry out denoising or, at least, one has to perform filtering more carefully than usually. Thus, it is desirable to predict efficiency of despeckling before starting this operation of SAR image processing [3].

One problem is that despeckling efficiency depends upon many factors [8, 9, 26]. They are properties (complexity) of an image to be processed, noise statistical and spatial correlation characteristics, availability and correctness of a priori information on noise characteristics, type of a used filter and its parameters as scanning window or block size, preset thresholds, etc. Thus, it is possible to characterize filtering efficiency in different ways. One way is to determine potential efficiency of filtering.

Currently there are several approaches to determining lower bounds of filtering efficiency [4, 5, 14, 17]. For the approach of Chatterjee and Milanfar [4], noise-free images are needed and potential (minimal) output mean square error (MSE) is determined for non-local filtering techniques under assumption that noise is additive, zero mean, white and its distribution is known a priori. Thus, despite of important results obtained in [4] (that will be briefly discussed below), this approach is impractical since noise-free image is not available for the considered task. The paper [5] puts forward a more practical approach where noise-free image is not anymore needed whilst determined lower bound agrees well with theory. However, the drawbacks of this approach are that it requires huge computations and determines not practical but potential output MSE.

The approach in [17] works for additive white Gaussian noise filtering based on local orthogonal transforms and the determined potential output MSE can differ from results in [4, 5] by up to 4 dB. Finally, the approach [14] proposed recently works well enough for white and spatially correlated additive noise with known variance. It produces a good estimate of output MSE provided by the best known filters for images that can be modeled by fractal Brownian motion (fBm). However, the calculations should be rather intensive.

The results presented in the papers [4, 5, 14, 17] allow concluding the following. For a given variance of additive noise, output MSE values (both lower bound and practically reachable) are the largest for highly tex-

* e-mail: edu.rubel@gmail.com

tural images. For such images, the existing state-of-the-art filters provide output MSE values that are very close to lower bound ones, especially if noise is intensive [14, 12, 21]. However, for simpler structure images, potential output MSE is usually considerably smaller than practical. Thus, potential output MSE, if derived somehow, is useless for practice since it does not describe attainable filtering efficiency.

Other problems [12] are the following. First, the results in [4, 5, 14, 17] have been obtained for additive Gaussian noise and our interest here is in suppressing multiplicative non-Gaussian noise (speckle). Second, it is desirable to predict not only standard metrics (quantitative criteria) but also metrics that characterize visual quality of filtered images [12]. Third, to be useful in practice, prediction of despeckling (filtering) efficiency should be simple and fast enough (faster than filtering itself).

Of course, it is desirable to have a general prediction procedure applicable for different types of filters. But we understand that this desire cannot be satisfied now and concentrate below on filtering based on discrete cosine transform (DCT).

There are several reasons behind this. First, the DCT based denoising provides noise removal efficiency close to the best known filters (see simulation results in [12] for additive noise and in [7, 8] for speckle noise). Thus, if prediction for the DCT-based filter is accurate enough, this means that it can also serve as a rough prediction for other state-of-the-art filters. Second, several interesting steps towards predicting filtering efficiency have been done recently just for the DCT-based filter, namely, the standard DCT and the known BM3D filter [10] where the latter one is considered to be the state-of-the-art in removing additive white Gaussian noise.

These steps are the following. Based on simulation results in [17], it has been supposed in [19] that filtering efficiency characterized by the ratio of output MSE to variance of input AWGN can be predicted based on one out of two simple statistics of DCT coefficients in 8×8 pixel blocks, in particular, mean probability ($P_{2\sigma}$) that absolute values of DCT coefficients do not exceed doubled standard deviation of AWGN (2σ). It has been shown [20] that it is possible to predict other parameters characterizing filtering efficiency as, improvement of peak signal-to-noise ratio (IPSNR) and improvement of the visual quality metric PSNR-HVS-M [16] (IPHVS), both expressed in dB. Moreover, this can be done not only for AWGN but also for spatially correlated noise under condition that its spatial spectrum is a priori known or accurately pre-estimated.

Later, it has been shown [18] that prediction of IPSNR and IPHVS is possible for the case of DCT-based removal of signal-dependent noise (that has additive and quasi-poissonian components [1]) under condition that parameters of these components are known in advance or accurately estimated in advance (then, an algorithm of probability estimation is modified accordingly). It has been also determined that it is enough to estimate $P_{2\sigma}$ in non-overlapping blocks and/or to use, at least, 300...500 blocks placed randomly in probability estimation. This makes prediction by about two orders faster than even the standard DCT based filtering that employs two DCTs (direct and inverse) in fully overlapping blocks [11].

Here, it is worth recalling a general principle on how prediction is performed. A sufficient part of work is done off-line and in advance. The main goal of this work is to obtain an analytically described dependence of a parameter that characterizes filtering efficiency (e.g., IPSNR) on a statistical parameter that simultaneously characterizes image complexity and noise intensity (e.g., $P_{2\sigma}$). Having the corresponding dependence, one calculates an input parameter (e.g., $P_{2\sigma}$), substitutes it into the obtained dependence as argument, and gets an estimate of a parameter that characterizes filtering efficiency (e.g., IPSNR).

Such dependences are obtained in advance by forming a scatter-plot for pairs of the considered parameters for a wide set of test images and noise parameters and fitting a curve into this scatter-plot [18, 19, 20]. Quality of such a fitting (and quality of prediction) is characterized by several statistical criteria [2]. To make prediction quite general and accurate, several actions have to be performed. First, it is possible to optimize (or to properly select) the parameter (probability) [22] employed as input parameter in prediction. In this sense, the probability $P_{0.5\sigma}$ (that absolute values of DCT coefficients do not exceed 0.5σ) has occurred [22] to be slightly better than $P_{2\sigma}$ and earlier used $P_{2.7\sigma}$. Second, selection of the test image set and a set of noise parameters influences fitting (argument values have to cover all possible interval and they have to be "equally sparsely" located). Third, a function chosen for fitting (polynomial, exponent, etc) also has an impact on fitting results. Thus, special attention has to be paid to this aspect with several trials and choosing a best version. Fourth, prediction using only one input parameter can be not accurate enough [22, 23]. Without essential loosing of computational efficiency and simplicity of prediction, it is possible to use two or more input parameters combined in some manner, in particular, using a trained neural network [23].

Therefore, here we deal with considering several tasks. The main of them is to analyze applicability of the prediction approaches to the case of despeckling SAR images where speckle is treated as a specific type of signal-dependent noise, which has been earlier discussed very briefly in [3]. Besides, we also aim to analyze possibilities of improving prediction accuracy.

The paper structure is the following. The second section describes the denoising mechanism of the DCT-based filter. The third section "Standard Methodology of Prediction" introduces used statistical parameters and a method for prediction. Section "Advanced Meth-

odologies of prediction" deals with improved methods of predicting by multi-parameter fitting and neural network learning. The last section analyses the obtained results of prediction for real aerial images and different methods.

DCT-based filtering and its modifications different noise types

DCT-based filter has high denoising efficiency and low computational complexity [17]. Moreover, it has been shown [17] that the DCT-based filter demonstrates efficiency close to the best-known filters (such as BM3D) [10] and to potential denoising bounds [4] particularly for AWGN model:

$$I_{an}^{add}(i,j) = I_t(i,j) + N_{Gaussian}(\sigma), \quad (1)$$

where I_t is true image I_{an}^{add}, is noisy image, i and j are indices of pixels in image. $N_{Gaussian}$ denotes zero mean additive white Gaussian noise (i.e., a 2D realization of Gaussian random process) with standard deviation of the noise σ.

Here, a basic block-wise denoising mechanism of the DCT filter is given for the AWGN case. After direct 2D DCT in a block, the following operation is carried out:

$$\mathrm{B}_{out}^{add}(n,m) = \begin{cases} B_{in}^{add}(n,m) \leftarrow B_{in}^{add}(n,m) > \beta\sigma, \\ 0 \leftarrow B_{in}^{add}(n,m) \le \beta\sigma, \end{cases} \quad (2)$$

where β is a denoising thresholding parameter that, in general, can vary in the range 2...4 (the recommended value is 2.7), n and m are spatial frequency indices in an image 8×8 pixels block, B_{in}^{add} denotes DCT coefficients of input noisy image block, B_{out}^{add} denotes DCT coefficients after thresholding. Then, inverse 2D DCT is carried out for B_{out}^{add}. The standard DCT-based filter [17] performs full-overlapping block-wise denoising and, at the final stage, it collects data from overlapping blocks together with averaging the filtered values for a given pixel.

However, for SAR remote sensing imagery, speckle which is a multiplicative nature noise-like phenomenon is more inherent. For one-look or single-look remote sensing images [24], the following model of multiplicative Rayleigh distributed speckle is considered adequate (for amplitude images) [15]:

$$I_{sdn}^{1-look}(i,j) = I_t(i,j) N_{Rij}(k), \quad (3)$$

where $N_{Rij}(k)$ denotes Rayleigh distributed random value, k is distribution parameter that provides unity mean, I_{sdn}^{1-look} is an (one-look noisy) image distorted by specific signal-dependent noise. Multi-look SAR images, i.e. averaged (by pixels) sets of images of the same sensed surface region, have slightly different kind of noise. Such noisy images can be modelled as averaged value of L Rayleigh noise realizations:

$$I_{sdn}^{L-look}(i,j) = \sum_{l} I_t^l(i,j) N_{Rij}^l(k) \Big/ L = I_t(i,j) \overline{N}_{Rij}, \quad (4)$$

where L means the number of image looks, I_{sdn}^{L-look} is the distorted multi-look image, $N_{Rij}^l(k)$ is l-th realization of unity mean Rayleigh random variable.

It is seen from (2) that denoising mechanism of the DCT filter deals with hard thresholding. For different noise types and models, denoising threshold is set differently. For multiplicative spatially uncorrelated noise case such as speckle, the denoising threshold is modified as:

$$\mathrm{B}_{out}^{mult}(n,m) = \begin{cases} B_{in}^{mult}(n,m) \leftarrow B_{in}^{mult}(n,m) > \beta\sigma_\mu \overline{S}_{in}^{mult}, \\ 0 \leftarrow B_{in}^{mult}(n,m) \le \beta\sigma_\mu \overline{S}_{in}^{mult}, \end{cases} \quad (5)$$

where $\overline{S}_{in}^{mult}$ is mean intensity of a given image block (that can be also measured in spatial domain), σ_μ^2 denotes (relative) variance of multiplicative noise, other introduced notations as B_{in}^{mult} and B_{out}^{mult} are similar to the ones earlier used in (2). Note that σ_μ^2 for the model (3) equals to 0.273 and it becomes σ_μ^2/L for multi-look amplitude images [15].

Standard Methodology of Prediction

Due to simplicity, high performance and easy adaptivity of the DCT-based filter to different types of the noise, this denoising technique is attractive for practical use. Being equipped by an efficiency prediction operation, it becomes even more attractive. However, prediction should be a simple and fast procedure. It is worth stressing here that remote sensing systems are demanding to computational complexity of data processing like denoising. Quite many recently proposed filters have high complexity [10] and, meanwhile, they can introduce essential distortions into processed images in some case, which is undesirable.

One of the purposes of denoising efficiency prediction is "catching" practical situations when filtering efficiency is not appropriate and the filtering procedure could be cancelled or avoided. The second goal is prediction of metric improvement (these can be metrics PSNR or PSNR-HVS-M [16]) without a corresponding reference image.

The principal idea of getting a predicted value consists in using some operation with some input statistics of a noisy image and further obtaining of the output (predicted) value. Thus, two tasks arise: what statistical parameter(s) to use and how to predict, i.e. to link two values – a statistical parameter(s) and a metric of denoising efficiency.

The abovementioned goals of prediction require low complexity of prediction operation and appropriate accuracy. This restricts a set of techniques and parameters that can be applied. It is preferable if only simple arithmetic operations are used for the purpose of prediction. Moreover, amount of statistics obtained from

an image for predicting the efficiency of its filtering can be also limited. This means that we need some informative local estimates that produce reasonably small volume of data.

The first task is strictly connected with the denoising mechanism of the DCT-based filter. This mechanism removes coefficients that are smaller than the preset threshold(s). It is a reasonable idea that the number of removed (zeroed) DCT coefficients strictly influences final denoising efficiency. In [19], the first steps of predicting the DCT-based filter efficiency were done. The proposed method uses hard thresholding operation and requires adequate threshold value setting. As statistical parameter, probability that DCT coefficients potentially are removed or not by the filter is used.

The proposed method collects local estimates for all considered image blocks using the procedure described above for subsequent prediction. Local statistical estimates for additive noise (AWGN) and multiplicative noise (speckle) models could be the following:

$$E_{out}^{add}(n,m,q)=\begin{cases}1 \leftarrow B_{in}^{add}(n,m,q)<\alpha\sigma,\\ 0 \leftarrow B_{in}^{add}(n,m,q)\geq\alpha\sigma,\end{cases} \quad (6)$$

$$E_{out}^{mult}(n,m,q)=\begin{cases}1 \leftarrow B_{in}^{mult}(n,m,q)>\alpha\sigma_{\mu}\bar{S}_{in}^{mult},\\ 0 \leftarrow B_{in}^{mult}(n,m,q)\leq\alpha\sigma_{\mu}\bar{S}_{in}^{mult},\end{cases} \quad (7)$$

$$P_{\alpha\sigma}(q)=\sum_{n,m}E_{out}(n,m,q)\Big/63, \quad (8)$$

where q is an index of an analyzed block, α is the thresholding parameter used for prediction (it is similar to β), $P_{\alpha\sigma}(q)$ is a set of local probability estimates calculated for the q-th block in a processed image.

Note that $P_{\alpha\sigma}(q)$ is calculated for 63 coefficients (in 8×8 pixel block) excluding DCT coefficient that corresponds to mean intensity and has indices (0. 0 – left up corner) in block (this coefficient is also not used in denoising). It is seen that the values of the local estimates of $P_{\alpha\sigma}(q)$ lie in the range 0...1. It is not a problem to remember and store the set of local estimates for a given image at intermediate stage of prediction.

Then, this set can be represented as some distribution. In [19], only mean value $\left(\bar{P}_{\alpha\sigma}=\sum P_{\alpha\sigma}(q)\right)$ was used for predicting the ratio MSE/σ^2. Thresholds for probabilities obtaining were 2σ and 2.7σ. The first threshold is used for estimation of probability that DCT coefficients do not exceed threshold. The second threshold was estimated in [19] the opposite way $\bar{P}_{2,7\sigma}=\sum\left(1\text{-}P_{2,7\sigma}(q)\right)$.

Motivations for using those thresholds were empirical and they followed from our previous experience. The threshold 2σ is usually exploited in the well known sigma-filter [13] for defining a neighbourhood whilst the threshold 2.7σ has been intensively used in DCT-based filtering [17].

For linking MSE/σ^2 and mean probability value for both thresholds, polynomial and exponential fitting functions were used. The prediction method was exploited both for DCT-based filter and BM3D. Function coefficients were calculated by maximizing goodness of fit (R^2) as fitting criteria:

$$R^2=1-SS_{res}/SS_{tot}, \quad (9)$$

where SS_{res} denotes the sum of squares of residuals, also called the residual sum of squares, SS_{tot} is the total sum of squares which is proportional to the sample variance. Traditionally, the goodness of fit is the main quantitative parameter that describes effectiveness (quality) of fitting.

Due to the fact that the studies in [19] were at initial stage, they have several drawbacks. First, a small number of test images was exploited. Thus, an insufficient number of scatter-plot points has been used in curve fitting. In particular, $\bar{P}_{2.7\sigma}$ and $\bar{P}_{2.\sigma}$ that correspond to texture images were not presented at scatter-plots. This means that, in general, a large set of points (different values of statistical parameter distributed along full range of possible parameter and metric values) must be used for accurate prediction.

In [20], as prediction model, exponent fitting function was used as the most suitable:

$$Metric_{pred}=a\exp\left(b\bar{P}_{\alpha\sigma}\right), \quad (10)$$

where $Metric_{pred}$ is a predicted value of a metric of denoising efficiency, a and b are coefficients of fitting function. As it has been mentioned before in [19], the cases of a equal to 2 or to 2,7 have been considered.

In [19], a larger (sufficient) number of points (34) was used and another noise model was considered – additive spatially correlated noise. Alongside with MSE/σ^2, fitting functions for improvement of the metrics PSNR and PSNR-HVS-M (the latter metric is based on human vision system and adequately assesses visual quality) were obtained for three noise models. The obtained approximations for spatially correlated noise turned out to be close to the approximations for the AWGN case. Partially this observation indicates universality of the proposed method that can be applied to other noise models. Due to it, we assume that prediction model based on AWGN can be applied to prediction of speckle removal efficiency and compared with those based on speckle-noised data.

New results of as threshold setting for prediction procedure were obtained in [22]. In addition, it has been shown that using the mean probability $P_{0,5a}$ (i.e. $\alpha=0.5$) is more suitable than $\bar{P}_{2\sigma}$ for prediction, i. e. providing higher goodness of fit value.

In Fig. 1, scatterplots of AWGN data for IPSNR and IPSNR-HVS-M metrics vs probabilities $\bar{P}_{2\sigma}$ and $\bar{P}_{0,5\sigma}$ are presented (blue points). For prediction performing, a large set of test images has been used: 128 different images and 10 noise levels (variances of AWGN were 4,

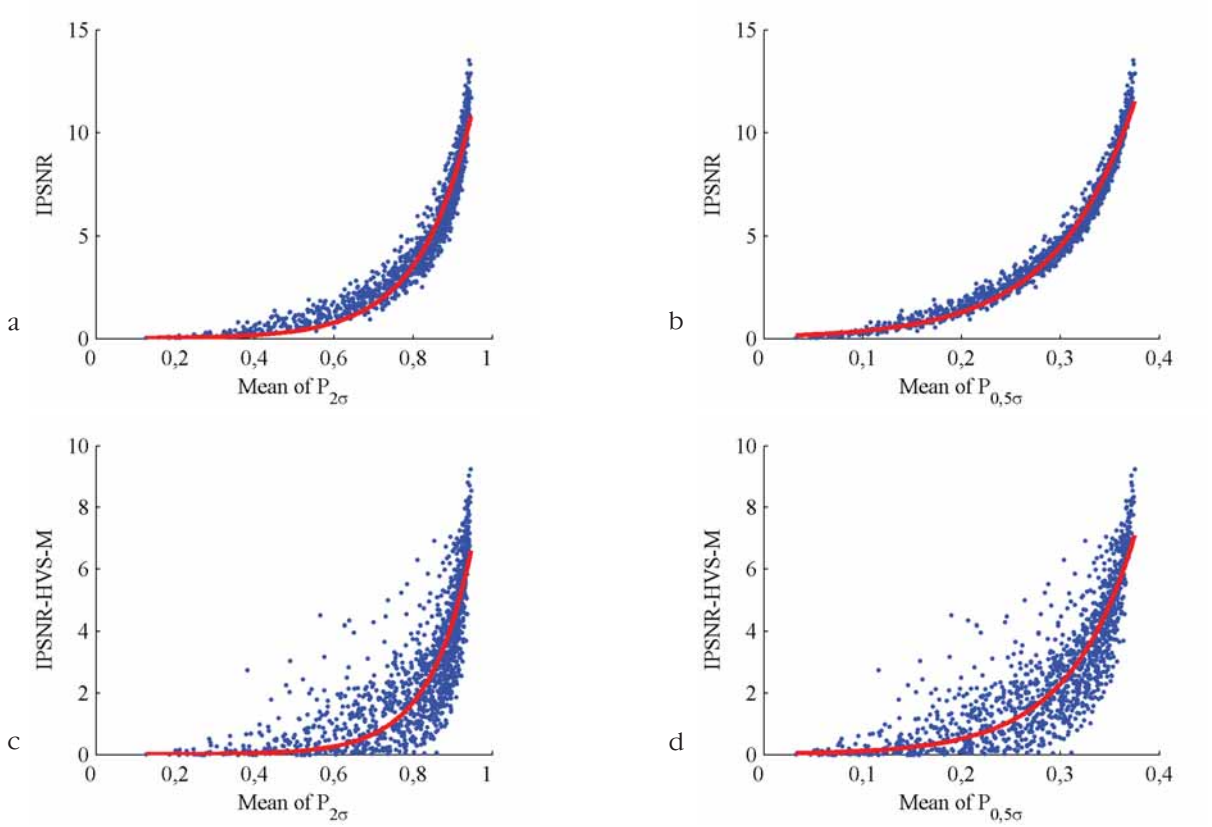

Fig. 1. 1D scatterplots of improvement of PSNR (a, b) and PSNR-HVS-M (c, d) for the DCT-based denoising vs mean of local estimates of $P_{2\sigma}$ (a, c) and $P_{0,5\sigma}$ (b, d) and the fitted 1D prediction functions (approximations)

9, 25, 64, 100, 144, 225, 289, 400, and 625). All used images have different content and are taken from different databases (TID2013 [6], USC-SIPI [25] and some other).

In addition, fitted curves of the exploited exponential fitting function (10) are shown as red lines. Coefficients of fitting functions and goodness of fit parameters are presented in Tables 1 and 2. It is well seen from the plots that IPSNR data points are less scattered than IPSNR-HVS-M data points. As a result, goodness of fit values for IPSNR functions are higher than for IPSNR-HVS-M. This means easier prediction for the IPSNR metric compared to the metric IPSNR-HVS-M. Also it should be stressed that the use of $\overline{P}_{0,5\sigma}$ is more preferable than the use of $\overline{P}_{2\sigma}$ since this reduces data scattering (R^2 occurs to be larger).

Besides, the scatterplots for IPSNR-HVS-M show that the proposed one-parameter (mean of $P_{\alpha\sigma}$) fitting model and, respectively, prediction can be not sufficiently accurate. Thus, it is desirable to apply some more advanced technique, primarily to IPSNR-HVS-M prediction. This can be done using more informative statistics as statistical parameter (-s) and appropriate predicting models.

Advanced Methodologies of Prediction

As it has been shown in the previous section, after procedure of local estimation of $P_{\alpha\sigma}$, a set of estimates having a certain distribution is obtained. Four examples of such distributions for two noisy images and two probabilities $P_{2\sigma}$ and $P_{0,5\sigma}$ are presented in Fig. 2. The used images are remote sensing single-look images distorted by speckle with relative variance σ_μ^2 equal to

Table 1
Coefficients of 1D fitting functions using statistical parameters obtained from AWGN-distorted data and goodness of fit results

	$P_{2\sigma}$		
Metric	a	b	R^2
IPSNR	$7.97*10^{-3}$	7.62	0.94
IPSNR-HVS-M	$0.99*10^{-3}$	9.31	0.72
	$P_{0,5\sigma}$		
Metric	a	b	R^2
IPSNR	0.11	12.53	0.98
IPSNR-HVS-M	$26*10^{-3}$	14.99	0.78

Table 2
Coefficients of the 2D fitted functions for the parameters obtained for AWGN case and goodness of fit results

	$P_{2\sigma}$			
Metric	a	b_1	b_2	R^2
IPSNR	$2.5*10^{-3}$	8.84	13.37	0.98
IPSNR-HVS-M	$4.29*10^{-6}$	15.06	55.9	0.91
	$P_{0.5\sigma}$			
Metric	a	b_1	b_2	R^2
IPSNR	$84.95*10^{-3}$	12.9	17.71	0.94
IPSNR-HVS-M	$1.4*10^{-3}$	20.66	201.6	0.86

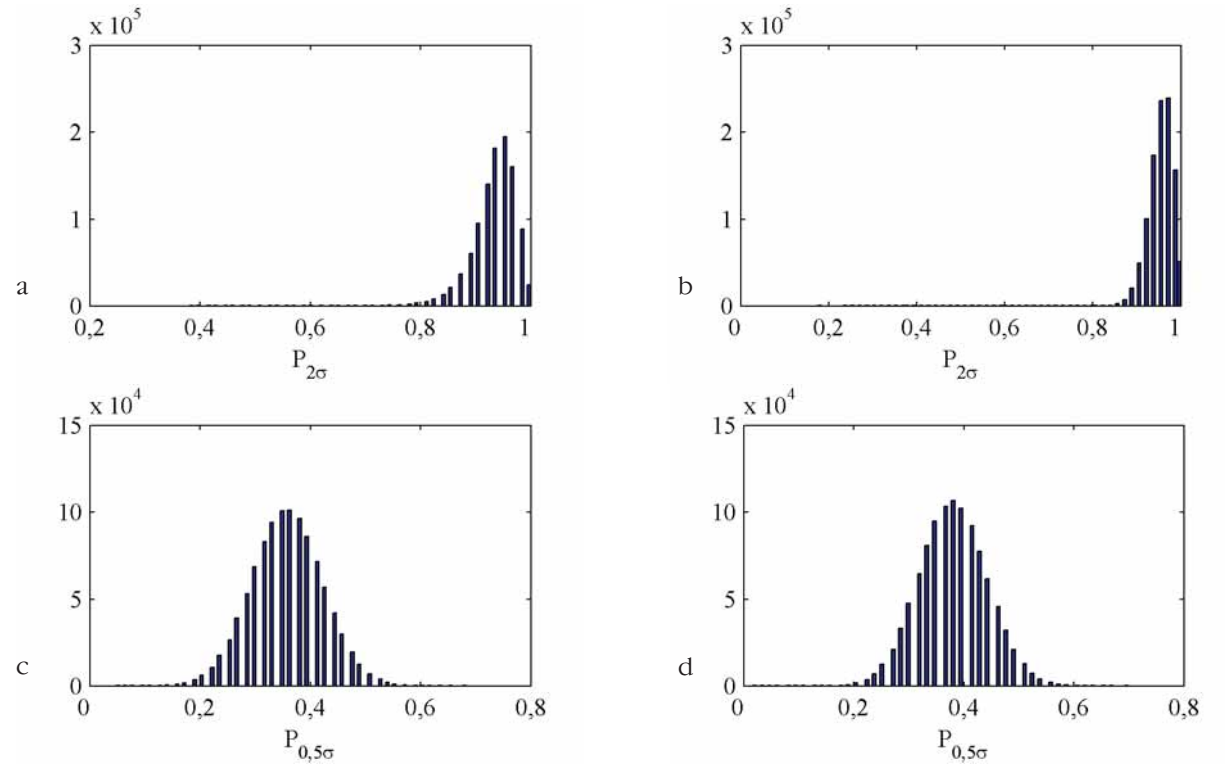

Fig. 2. Histograms of local estimates of $P2_\sigma$ (a, b) and $P_{0,5\sigma}$ (c, d) for first test image (a, c) and for second (b, d)

0.273 produced by Rayleigh noise with . $P_{\alpha\sigma}(q)$ are obtained using expressions (7) and (8).

Achieved improvements of metrics for denoising by the DCT-based filter are the following: for the the test image №16, IPSNR is 10.03 dB and IPSNR-HVS-M is 6.16 dB; for the image № 38, improvements are essentially larger: IPSNR is 16.71 dB and IPSNR-HVS-M is 12.03 dB (the mentioned test images are presented later in Fig. 4) and a larger positive effect due to filtering should be observed.

Meanwhile, the mean probabilities of $P_{2\sigma}$ and $P_{0,5\sigma}$ for these two test images are close: 0.934 and 0.359 for first test image; 0.953 and 0.381 for the second test image. They lie in the range where the fitted curves are changing rapidly (see Fig. 1). Therefore, for such case, prediction error can be large if a used input statistic parameter would be estimated with inappropriate accuracy. Thus, more input information for prediction procedure can be needed.

Such information can be obtained (retrieved) from the sample (set) of local estimates. In [20], instead of considering only the mean value, six first order statistic parameters were exploited for AWGN data: the mean (M), median (Med), mode (Mod), variance (D), skewness (S) and kurtosis (K). Extended exponential function that depends on these six parameters in exponent was proposed due to its simplicity and convenience:

$$Metric_{pred} = a\exp\left(\sum_i b_i O_i(P_{\alpha\sigma})\right), \qquad (11)$$

where $Metric_{pred}$ is the predicted value of metric, a and b_i are coefficients of fitting functions, O_i is a statistical operator for estimating parameters of the distribution of local estimates of $P_{\alpha\sigma}$.

It has been shown that joint use of, at least, M and D provides higher predicting performance than the standard procedure for the metric IPSNR-HVS-M. The use of three or more statistics parameters for the exponential model (11) results in insignificant improvement of prediction performance. Thus, the use of only M and D in (12) can be considered sufficient and such a prediction has low computational cost. Moreover, it has been shown that the prediction procedure does not require full-overlapping processing and 300...500 is the sufficient number of blocks where local estimates have to be obtained.

$$Metric_{pred} = a\exp(b_1 M(P_{\alpha\sigma}) + b_2 D(P_{\alpha\sigma})). \qquad (12)$$

In Fig. 3, the corresponding 2D scatterplots with the fitted surfaces are presented for mean and variance of local estimates of $P_{2\sigma}$ and $P_{0,5\sigma}$. The obtained parameters of the 2D fitting surfaces are presented in Tables 3 and 4.

Desire to further improve prediction (e.g., using more than two statistical parameters) leads to more advanced prediction procedure [23]. The fitting model is, in fact, based on feed-forward neural network (NN) with three layers (with empirically chosen number of neurons) that was trained for approximating a dependence. The NN has the number of inputs equal to the number of used input statistical parameters, ten neurons in hidden layer and one output neuron for providing a predicted value. A network training function, which up-

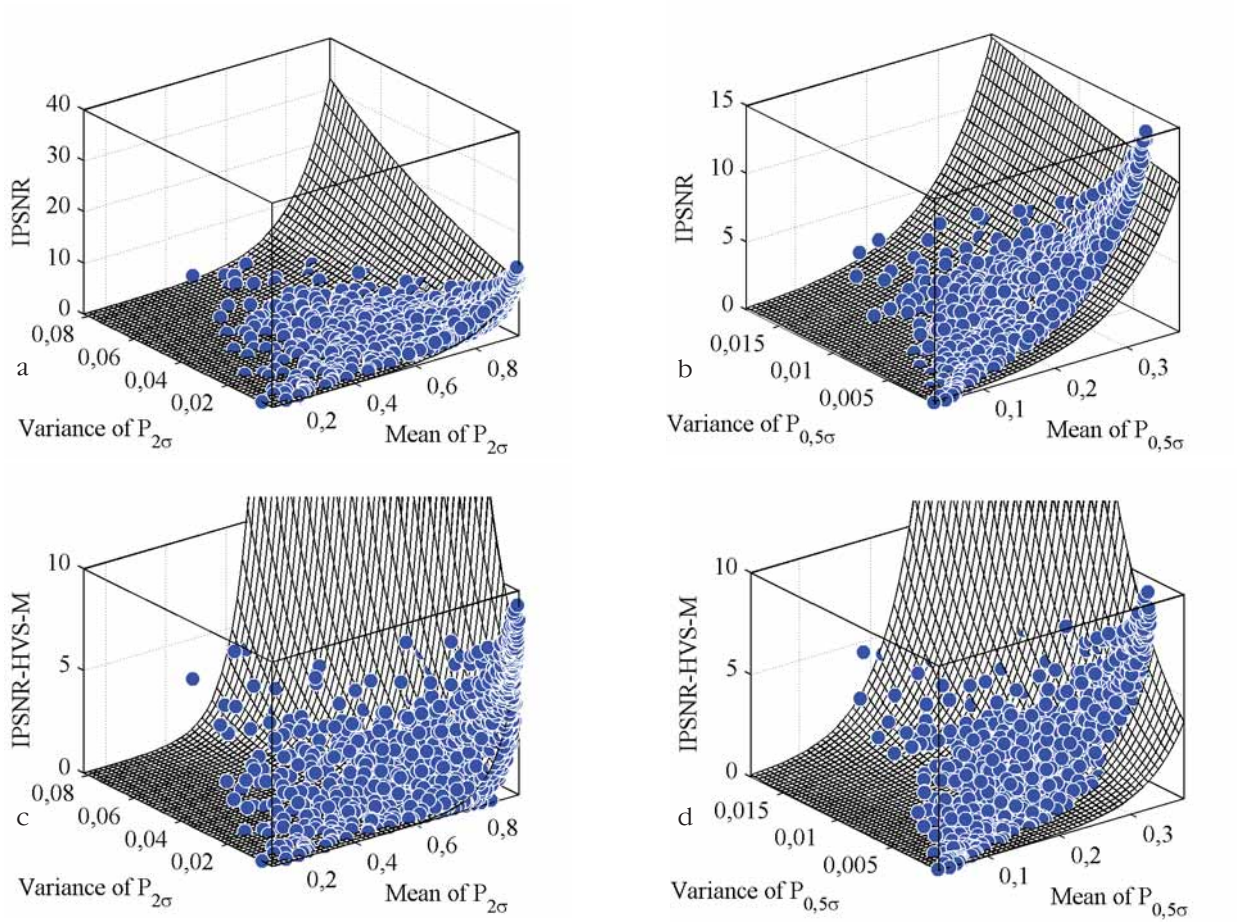

Fig. 3. 2D scatterplots of improvements of PSNR (a, b) and PSNR-HVS-M (c, d) of the DCT-based denoising on statistical parameters (mean and variance) of local estimates of $P_{2\sigma}$ (a, c) and $P_{0.5\sigma}$ (b, d) and the fitted 2D prediction (approximation) functions

dates values, was used according to Levenberg-Marquardt optimization algorithm that is based on least-squares algorithm.

It has been shown in [23] that prediction is good if one use, at least, four input parameters: M, D, S and K. The standard deviation of actual practical prediction error for IPSNR-HVS-M was about 0.5 dB where such variation of the metric value is practically undistinguishable for a human eye. One reason why such a high accuracy is provided is that four aforementioned parameters are informative and not essentially inter-connected (for instance, Med and Mod are strongly connected with M and their joint usage would be inefficient).

Here we would like to answer the following question: is it possible to use a fitting function and NN trained for AWGN data for predicting denoising efficiency for speckle images or it is worth using speckled images and data for them in NN training and/or in function fitting.

Previously, 128 images distorted by 10 levels (noise variances) of AWGN were used for the NN-predictor as well as for one- and two-parameter fitting. To verify the proposed methods for speckle case, all 128 images are modelled as multi-look images (from 1 to 10 looks) to provide different relative variances. Such a large number of images are used for providing full-range statistics for effective prediction. Speckle-distorted data (1280 points) are exploited by three previously described methods: one-parameter fitting (using only M parameter of $P_{\alpha\sigma}$), two-parameter fitting model (using parameters M and D of P_{as}) and NN-predictor (using the parameters M, D, S and K of $P_{\alpha\sigma}$).

Here the analysis of the proposed method performance, i.e. goodness of fit, is provided. Goodness of fit results for function fitting models and NN-predictor learned for AWGN and speckle cases are presented for $P_{2\sigma}$ and $P_{0.5\sigma}$ in Tables 3. It is well seen that fitting for AWGN-distorted data gives higher goodness of fit than for speckle-distorted data. That is observed for all methods and probabilities.

IPSNR fitting results are very good for all methods using AWGN-distorted data. Satisfactory results for IPSNR-HVS-M can be achieved by using two-parameter function and NN-predictor also using AWGN-distorted data. For speckle-distorted data, IPSNR values can be well predicted by two-parameter fitting and NN-predictor. However, IPSNR-HVS-M predicting using speckle data can be well only by using NN-predictor.

Note that satisfactory R^2 values for $P_{0.5\sigma}$ are higher for all methods and exploited data than for $P_{2\sigma}$. It should be stressed that R^2 values increase by using more statistical parameters and more complicated predicting

Table 3
Goodness of fit R2 for different prediction methods using statistical parameters

$P_{2\sigma}$			
Metric	One-parameter fitting	Two-parameter fitting	Multi-parameter NN
AWGN-distorted data			
IPSNR	0.94	0.94	0.97
IPSNR-HVS-M	0.72	0.86	0.95
Speckle-distorted data			
IPSNR	0.54	0.81	0.9
IPSNR-HVS-M	0.42	0.65	0.87
$P_{0.5\sigma}$			
Metric	One-parameter fitting	Two-parameter fitting	Multi-parameter NN
AWGN-distorted data			
IPSNR	0.98	0.98	0.99
IPSNR-HVS-M	0.78	0.91	0.96
Speckle-distorted data			
IPSNR	0.69	0.88	0.92
IPSNR-HVS-M	0.54	0.74	0.90

models. As result, the NN-predictor using $P_{0.5s}$ has the highest R^2 value for AWGN- and speckle-distorted data.

However, one of above mentioned requirements for prediction methods is low computational cost. Statistical parameters that are used for prediction are simply calculated. One- and two- parameter function fitting are also very simple predicting models. These methods require fitting operation, i.e. learning for certain data (for some denoising technique or noise model). Input parameters easily are inserted into the corresponding fitting function with the known coefficients. Hence, prediction procedure using fitting functions is very fast procedure. It can be easily applied in remote sensing systems due to their computational restrictions.

The NN-predictor is more complicated since it requires some additional software and support. As well as fitting models, NN-predictor also requires one training procedure on corresponding data. It requires more statistics due to providing higher predicting performance by using more advanced generalization ability than function fitting models. Besides, such complexity increases computational burden. That restricts this method applying in some image acquisition systems.

Analysis of the obtained results

Observing previous fitting results, AWGN-learned prediction methods can be applied to multi-look remote sensing images distorted by speckle. That can prove universality of prediction approaches using AWGN data for prediction denoising efficiency for other noise model. Two-parameter fitting method and NN-predictor are used for prediction verification on real remote sensing images.

For verification, 40 remote sensing images are used as the test set, some test images are shown in Fig. 4.

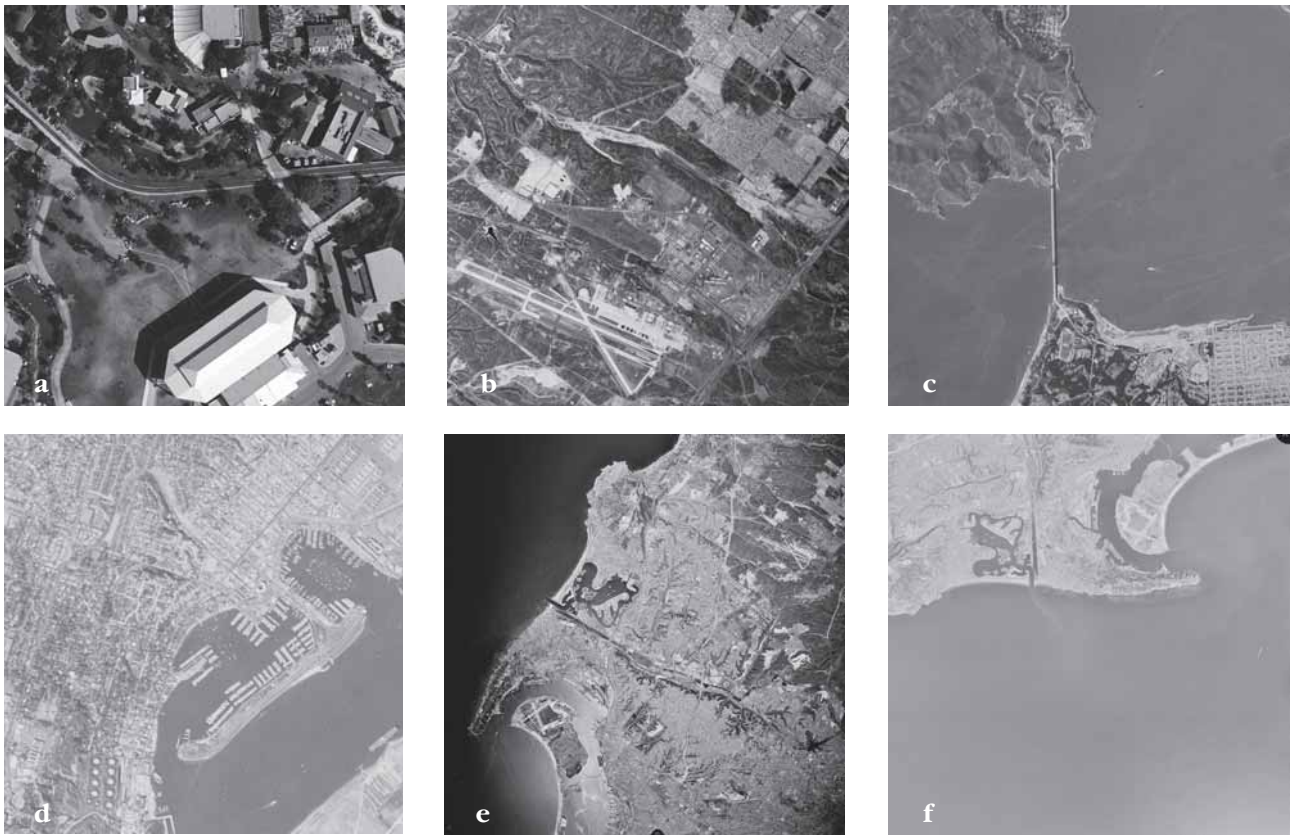

Fig. 4. Examples of the test aerial images: a – test image №1, b – №5, c – №7, d – №14, e – №16, f – №38

There are some widely used test images among them: fr01-04 (№1-4), San Diego (№5), Frisco (№7). Images have different sizes: from 512*512 to 1024*1024 pixels and are grayscale with 256 intensity levels. It is well seen that images have various content, e.g. textures, fine details, homogenous regions), and pixels size.

Practical denoising data and the predicted values for IPSNR and IPSNR-HVS-M are shown in Figs 5 and 7 for AWGN data. In Figs 6 and 8, the results for speckle data are presented. Different number of looks of remote sensing images are considered as examples: single, four and seven. Prediction methods learned by large datasets are verified by applying on real grayscale remote-sensing images. It is well seen that one-look images is the hardest case for prediction. Prediction using AWGN-distorted data is more effective performed by the NN-predictor than by two-parameter fitting for all metrics and data.

Prediction using NN and speckle data seems to be the most effective for one-look images. However, for multi-look images case, both AWGN and speckle learned methods are quite effective. This is an interesting observation: once the obtained data, e.g., AWGN-distorted, and the NN-predictor trained on it can be applied to some another noise model or model with unknown parameters.

Note that threshold setting (2σ or 0,5σ), i.e. input parameter choosing for prediction model, influences prediction performance. For instance, statistics obtained from test image №38 produce outliers for the NN- predictor if one uses $P_{2\sigma}$ whilst prediction using $P_{0,5\sigma}$ performs better.

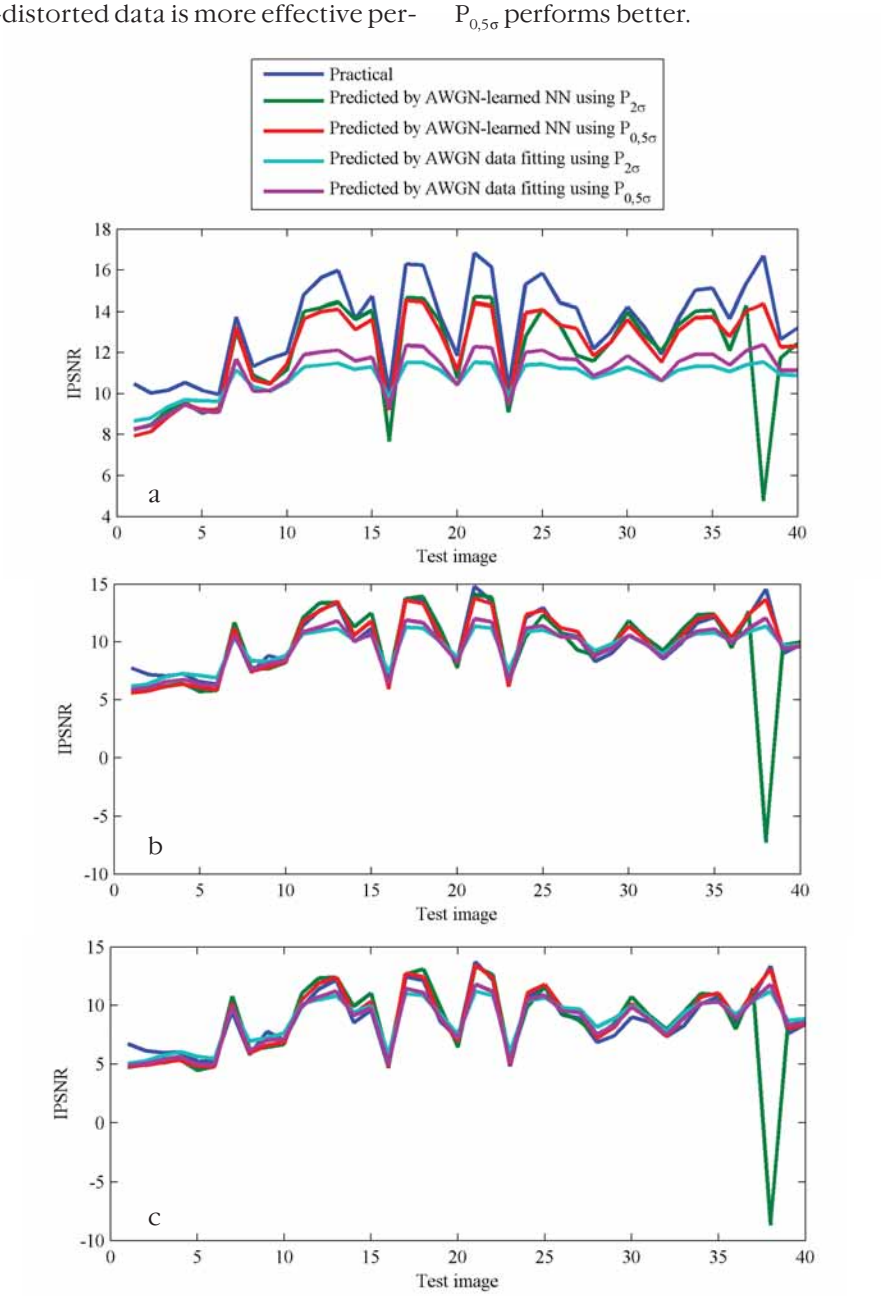

Fig. 5. Improvement of practical PSNR values for 1-look images (a), 4 -look images (b), 7-look images (c) processed by the DCT-based filter and the predicted results by fitting and NN based methods using statistical parameters of local estimates of $P_{2\sigma}$ and $P_{0,5\sigma}$ (for NN training and fitting, AWGN-distorted data were used)

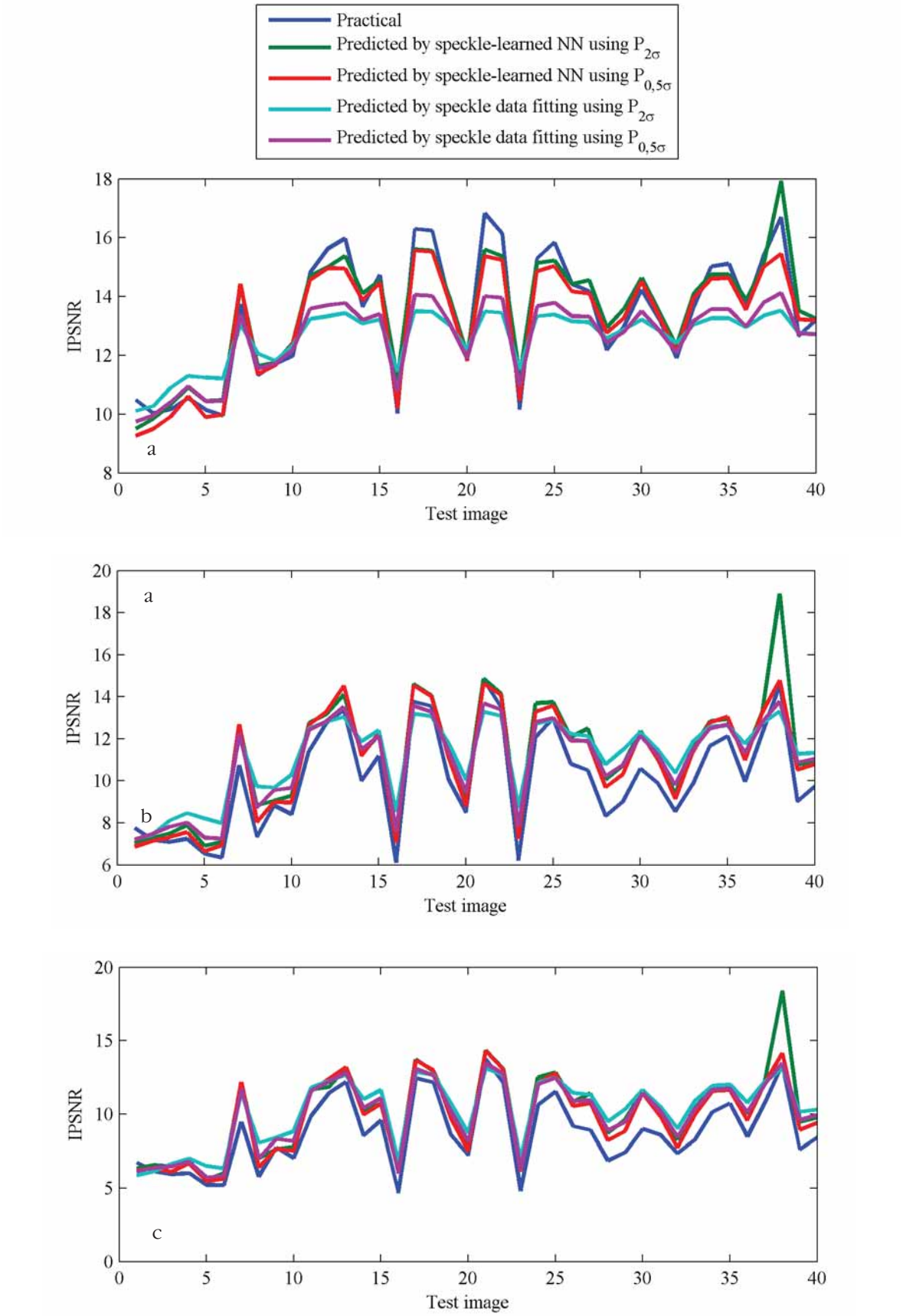

Fig. 6. Improvement of practical PSNR values for 1-look images (a), 4-look images (b), 7-look images (c) processed by the DCT-based filter and the predicted results by fitting and NN based methods using statistical parameters of local estimates of $P_{2\sigma}$ and $P_{0,5\sigma}$ (for NN training and fitting, speckle-distorted data were used)

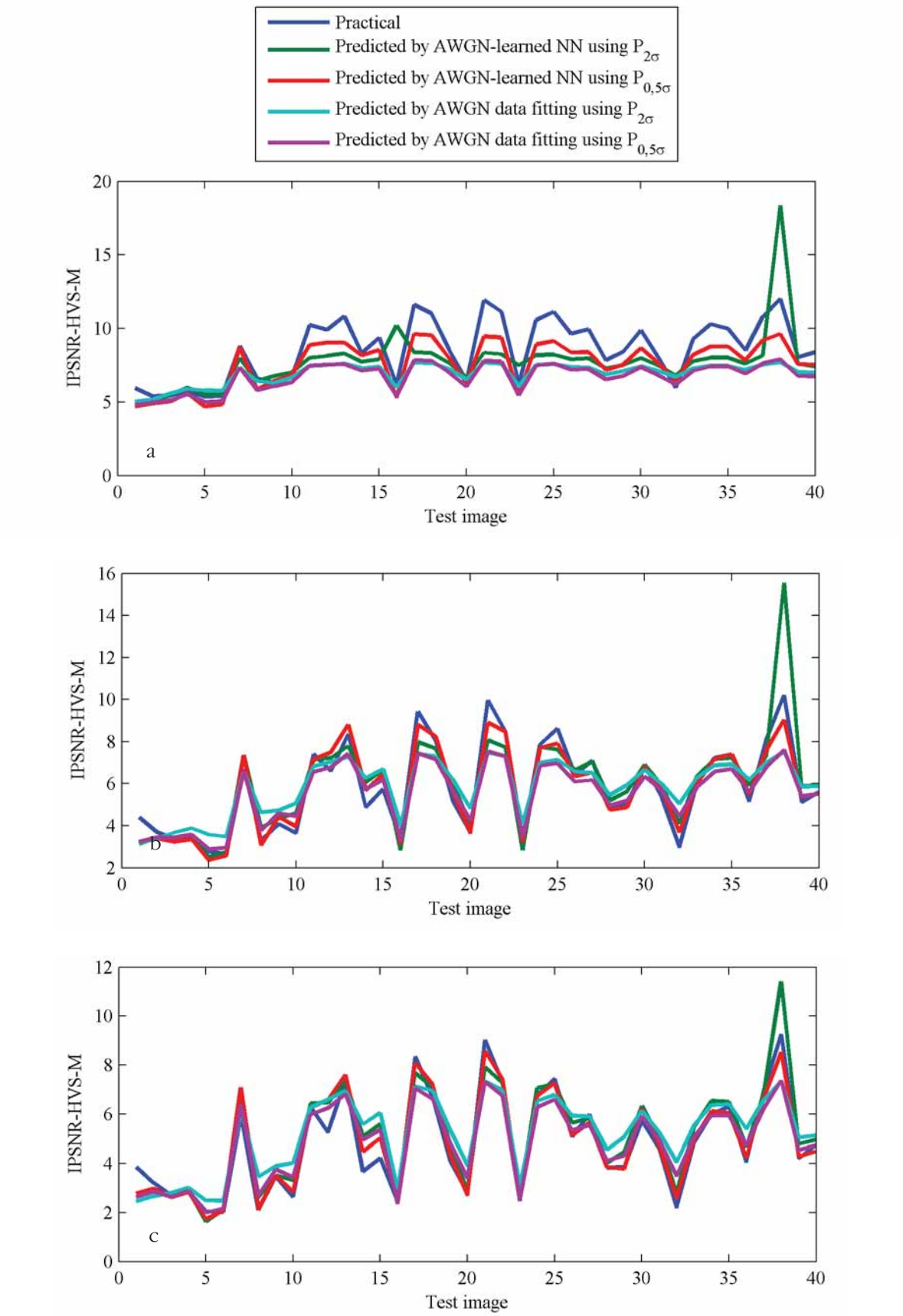

Fig. 7. Improvement of practical PSNR-HVS-M values for 1-look images (a), 4-look images (b), 7-look images (c) processed by the DCT-based filter and the predicted results by fitting and NN based methods using statistical parameters of local estimates of $P_{2\sigma}$ and $P_{0,5\sigma}$ (for NN training and fitting, AWGN-distorted data were used)

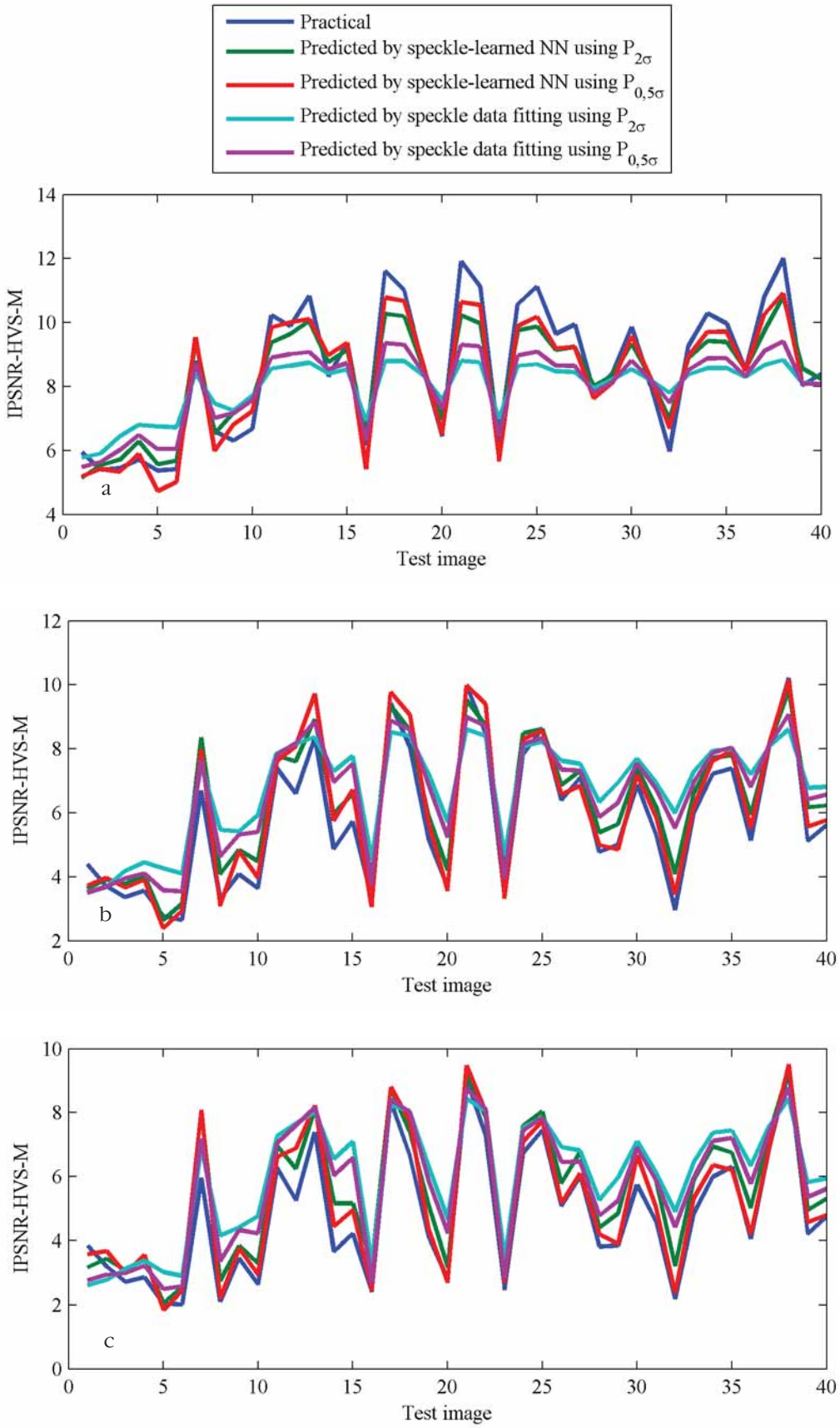

Fig. 8. Improvement of practical PSNR-HVS-M values for 1-look images (a), 4-look images (b), 7-look images (c) processed by the DCT-based filter and the predicted results by fitting and NN based methods using statistical parameters of local estimates of $P_{2\sigma}$ and $P_{0,5\sigma}$ (for NN training and fitting, speckle-distorted data were used

Table 4
Variances of errors in dB for prediction by different methods for 40 test aerial images

Prediction method	IPSNR		IPSNR-HVS-M	
	$P_{2\sigma}$	$P_{0.5\sigma}$	$P_{2\sigma}$	$P_{0.5\sigma}$
single-look images				
AWGN-learned two-parameter fitting	2.187	1.176	2.115	1.514
AWGN-learned multi-parameter NN	2.464	**0.257**	1.739	**0.426**
speckle-learned two-parameter fitting	1.846	0.997	1.929	1.142
speckle-learned multi-parameter NN	1.133	**0.274**	1.248	**0.324**
4-look images				
AWGN-learned two-parameter fitting	2.069	1.065	1.782	1.229
AWGN-learned multi-parameter NN	3.926	**0.331**	1.293	**0.293**
speckle-learned two-parameter fitting	1.662	0.849	1.588	0.901
speckle-learned multi-parameter NN	1.934	**0.238**	1.839	**0.189**
7-look images				
AWGN-learned two-parameter fitting	1.772	0.888	1.467	1.009
AWGN-learned multi-parameter NN	4.161	**0.387**	0.974	**0.289**
speckle-learned two-parameter fitting	1.386	0.699	1.312	0.763
speckle-learned multi-parameter NN	2.316	**0.263**	2.032	**0.232**

From analysis of the presented plots, some observations can be done:

1. The DCT-based filter applied to speckled images can provide significant improvement of visual quality (see, e.g., the IPSNR and IPSNR-HVS-M values for the test images №7, 11, 13, 17, 18, 21, 22, 24, 25, and 38 in Figs 5-8).

2. However, in some cases (see the data for the test images №5, 16, 20, 23 and 32 due to their complex content), the filter provides insignificant improvement of metrics.

3. It is well seen that differences between practical and predicted results reach about one dB for multi-look images (see Figs 5-8b, c) in some cases. For single-look images such differences are, on the average, larger (see Figs 5-8a).

4. Multi-look images have lower relative variance than single-look images due to (4). Therefore, enhanced multi-look images have higher visual quality.

In Table 7, MSE values of prediction errors for 40 test images dataset and different number of looks are presented. Let us summarize these results:

1. It is well seen that prediction error MSEs are smaller if $P_{0,5\sigma}$ is used for prediction. That is true for all prediction methods and metrics.

2. AWGN- and speckle-learned two-parameter fitting for multi-look images have larger error MSEs than NN-predictors.

3. For single- and multi-look images, AWGN- and speckle-learned NN-predictor using $P_{0,5\sigma}$ have appropriate error MSEs where RMSE values do not exceed 0,5 dB.

4. Speckle-learned NN are even better than AWGN-learned NN for multi-look images (see bold numbers). For single-look images and IPSNR metric, however, the situation is the opposite.

5. AWGN-learned NN can be applied to speckle-distorted images instead of speckle-learned NN without significant increasing of errors.

Besides, accuracy of denoising efficiency prediction provided by prediction methods and exploited by other automatic processing without human interaction have to be more accurate. Thus, our further work will be devoted to providing more accurate prediction for other noise models and denoising techniques.

Conclusions

Methodology of denoising efficiency prediction of the DCT-based filter is proposed. The proposed method estimates local statistics from image 8x8 pixel blocks in DCT domain. Transformed blocks are processed by hard thresholding procedure to provide local estimates of the considered probabilities. Local estimates are collected and their distribution parameter(s) is calculated. These can be sample mean or other simple statistics. These parameters are inputs for prediction model with output predicted metric (IPSNR and IPSNR-HVS-M) of denoising efficiency.

Two prediction models are exploited: fitting function model and feed-forward neural network (NN). It is shown that two-parameter function fitting model is very simple procedure with high prediction performance. In turn, the NN-predictor demonstrates the highest prediction performance using more statistics with more complicated prediction mechanism.

For prediction providing by the model fitting or by the NN training, a rather large data (image) set is needed. Images in this set can be distorted by noise of two models: AWGN or speckle. In general, it is possible to apply the models obtained for AWGN case to predicting speckle suppression efficiency in single and multi-look remote sensing images. This proves a certain universality of the proposed prediction approach. However, it is better to use images with simulated speckle at initial stage (curve fitting or NN training) and then to apply these results to images corrupted by speckle. The largest benefit is provided for one-look images.

Further works will be devoted to predicting denoising efficiency for other noise models and other denoising techniques.

References

1. Acito N. Signal-dependent noise modeling and model parameter estimation in hyperspectral images / N. Acito, M. Diani, G. Corsini // IEEE Transactions on Geoscience and Remote Sensing. – 2011. – Vol. 49. – No 8. – P. 2957-2971.
2. An R-squared measure of goodness of fit for some common nonlinear regression models / C. Cameron, A. Windmeijer, A. G. Frank, H. Gramajo, D. E. Cane, C. Khosla // Journal of Econometrics. – 1997. – Vol. 77. – No 2. – P. 329-342.
3. Approaches to Automatic Data Processing in Hyperspectral Remote Sensing / V. Lukin, S. Abramov, N. Ponomarenko, S. Krivenko, M. Uss, B. Vozel, K. Chehdi, K. Egiazarian, J. Astola // Telecommunications and Radio Engineering. – 2014. – Vol. 73. – No 13. P. 1125-1139.
4. Chatterjee P. Is Denoising Dead / P. Chatterjee, P. Milanfar // IEEE Transactions on Image Processing. – 2010. – Vol. 19. – No 4. – P. 895-911.
5. Chatterjee P. Practical Bounds on Image Denoising: From Estimation to Information / P. Chatterjee, P. Milanfar // IEEE Transactions on Image Processing. – May 2011. – Vol. 20. – No 5. – P. 1221-1233.
6. Color Image Database TID2013: Peculiarities and Preliminary Results / N. Ponomarenko, O. Ieremeiev, V. Lukin, K. Egiazarian, L. Jin, J. Astola, B. Vozel, K. Chehdi, M. Carli, F. Battisti, C.-C. Jay Kuo // 4th European Workshop on Visual Information Processing EUVIP2013, Paris, France. –2013. – 6 p.
7. Denoising of single-look SAR images based on variance stabilization and non-local filters / M. Makitalo, A. Foi, D. Fevralev, V. Lukin // Proceedings of MMET. – 2010. – 4 p.
8. Efficiency Analysis of Combined Despeckling of Single-Look SAR Images / R. A. Kozhemiakin, S. S. Krivenko, V. V. Lukin, R. C. P. Marques, F. N. S. de Medeiros, B. Vozel // Aerospace Engineering and Technology. – 2013. – Vol. 5. – No 102. – P. 102-111.
9. Exploiting patch similarity for SAR image processing: the nonlocal paradigm / C.-A. Deledalle, L. Denis, G. Poggi, F. Tupin, L. Verdoliva // IEEE Signal Processing Magazine, Recent Advances in Synthetic Aperture Radar Imaging. – 2014. – 8 p.
10. Image denoising by sparse 3-D transform-domain collaborative filtering / K. Dabov, A. Foi, V. Katkovnik, K. Egiazarian // IEEE Transactions on Image Processing. – 2007. – Vol. 16. – No 8. – P. 2080-2095.
11. Image filtering based on discrete cosine transform / V. Lukin, R. Oktem, N. Ponomarenko, K. Egiazarian // Telecommunications and Radio Engineering. – 2007. – Vol. 66. – No 18. – P. 1685-1701.
12. Image Filtering: Potential Efficiency and Current Problems / V. Lukin, S. Abramov, N. Ponomarenko, K. Egiazarian, J. Astola // Proceedings of ICASSP, Prague. – May 2011. – P. 1433-1436.
13. Lee J. S. Digital image smoothing and sigma filter / J. S. Lee // Computer Vision, Graphics and Image Processing. – 1983. – Vol. 24. – No 2. – P. 255-269.
14. Lower Bound on Image Filtering Mean Squared Error in the Presence of Spatially Correlated Noise / M. Uss, A. Rubel, V. Lukin, B. Vozel, K. Chehdi // IEEE: Proceedings of MRRS, Kiev, Ukraine. – 2014. – P. 10-13.
15. Oliver C. Understanding Synthetic Aperture Radar Images / C. Oliver, S. Quegan // SciTech Publishing. – 2004. – 486 p.
16. On between-coefficient contrast masking of DCT basis functions / N. Ponomarenko, F. Silvestri, K. Egiazarian, M. Carli, J. Astola, V. Lukin // Proceedings of the Third Int. Workshop on Video Processing and Quality Metrics, USA. – 2007. – Vol. 3. – 4 p.
17. Pogrebnyak O. Wiener discrete cosine transform-based image filtering / O. Pogrebnyak, V. Lukin // SPIE: Journal of Electronic Imaging. – 2012. – Vol. 21. – Is. 4. – 15 p.
18. Prediction of DCT-based Denoising Efficiency for Images Corrupted by Signal-Dependent Noise / S. Krivenko, V. Lukin, B. Vozel, K. Chehdi // Proceedings of IEEE 34th International Scientific Conference Electronics and Nanotechnology, Kiev, Ukraine. – 2014. – P. 254-258.
19. Prediction of Filtering Efficiency for DCT-based Image Denoising / S. Abramov, S. Krivenko, A.Roenko, V. Lukin, I. Djurovic, M. Chobanu // Proceedings of MECO, Budva, Montenegro. – 2013. – P. 97-100.
20. Rubel A. S. Prediction of Filtering Efficiency for Discrete Cosine Transform Based Removal of Additive Noise on Images / A. S. Rubel, V. V. Lukin // Radio-electronic and Computer Systems. – 2013. – Vol. 4. – P. 35-45.
21. Rubel A. Efficiency of DCT-based denoising techniques applied to texture images / A. Rubel, V. Lukin, O. Pogrebnyak // Proceedings of MCPR, Cancun, Mexico. – 2014. – P. 261-270.
22. Rubel O. An Improved Prediction of DCT-Based Filters Efficiency Using Regression Analysis / O. Rubel, V. Lukin // Information and Telecommunication Sciences, Kiev, Ukraine. – 2014. – Vol. 5. – No 1. – P. 30-41.
23. Rubel A. A Neural Network Based Predictor of Filtering Efficiency for Image Enhancement / A. Rubel, A. Naumenko, V. Lukin // Proceedings of MRRS, Kiev, Ukraine. – 2014. – P. 14-17.
24. Schowengerdt R. A. Remote Sensing: Models and Methods for Image Processing: Third edition / R. A. Schowengerdt / / Academic Press, San Diego, CA. – 2007. – 515 p.
25. The USC-SIPI Image Database. [Electronic resource] – Access mode: http://sipi.usc.edu/database/ – 2014.
26. Touzi R. A. Review of Speckle Filtering in the Context of Estimation Theory / R. A. Touzi // IEEE Trans. on GRS. – 2002. – Vol. 40. – No 11. – P. 2392-2404.

МЕТОДЫ ПРОГНОЗИРОВАНИЯ ЭФФЕКТИВНОСТИ ПОДАВЛЕНИЯ СПЕКЛ-ШУМА ДЛЯ ФИЛЬТРА НА ОСНОВЕ ДКП
В. В. Лукин, А. С. Рубель, А. В. Науменко, Б. Возель
Представлено и произведено сравнение нескольких методов прогнозирования эффективности подавления спекл-шума для ДКП фильтра. Представленные методы позволяют выполнять прогнозирование значений некоторых стандартных количественных критериев, например, возрастания пикового соотношения сигнал/шум (IPSNR) благодаря фильтрации так же успешно, как и значений некоторых критериев визуального качества отфильтрованных изображений. Исследованы точные автоматические процедуры прогнозирования, использующие моменты статистических параметров. Такие параметры рассчитываются в блоках размером 8*8 пикселей на изображениях, искаженных спекл-шумом с некоторыми характеристиками (количество взглядов), которые считаются априорно известными или вычисленными заранее с приемлемой точностью. Показана возможность применения методов для искаженных изображений при разном количестве взглядов. Прогнозирование на основе нейронной сети, обученной на предварительно полученных данных со спекл-шумом, является наиболее эффективным.
Ключевые слова: спекл-шум, дистанционное зондирование, ДКП фильтр, эффективность прогнозирования

МЕТОДИ ПРОГНОЗУВАННЯ ЕФЕКТИВНОСТІ ПРИДУШЕННЯ СПЕКЛ-ШУМУ ДЛЯ ФІЛЬТРА НА ОСНОВІ ДКП
В. В. Лукін, О. С. Рубель, О. В. Науменко, Б. Возель
Представлено та проведено порівняння декількох методів прогнозування ефективності придушення спекл-шуму для ДКП фільтра. Запропоновані методи дозволяють виконувати прогнозування значень деяких стандартних кількісних критеріїв, наприклад збільшення пікового співвідношення сигнал/шум (IPSNR) так же успішно, як і значень деяких критеріїв візуальної якості відфільтрованих зображень. Досліджені точні автоматичні процедури прогнозування, що використовують моменти статистичних параметрів. Такі параметри розраховуються в блоках розміром 8*8 пікселів на зображеннях, спотворених спекл-шумом з деякими характеристиками (кількість поглядів), які вважаються апріорно відомими або обчисленими заздалегідь із прийнятною точністю. Показана можливість застосування методів для спотворених зображень при різній кількості поглядів. Прогнозування на основі нейронної мережі, навченої на заздалегідь отриманих даних зі спекл-шумом, є найбільш ефективним.
Ключові слова: спекл-шум, дистанційне зондування, ДКП фільтр, ефективність прогнозування